Supporting Information: K-doped $FeOOH/Fe_3O_4$ nanoparticles gown on stainless steel substrate with superior and increasing specific capacity

*Haiqiang Luo, Keyu Tao and Yun Gong**

Department of Applied Chemistry, College of Chemistry and Chemical Engineering,

Chongqing University, Chongqing 401331, P. R. China.

*Corresponding author's email: gongyun7211@cqu.edu.cn

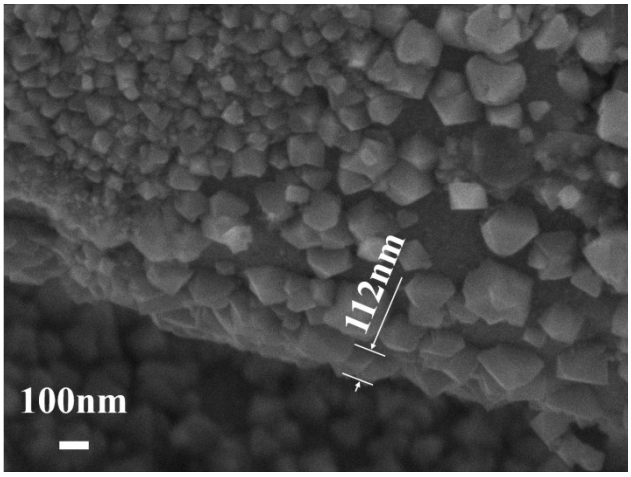

Figure S1 Cross section image of K-doped FeOOH/Fe_3O_4/SS.

(a)

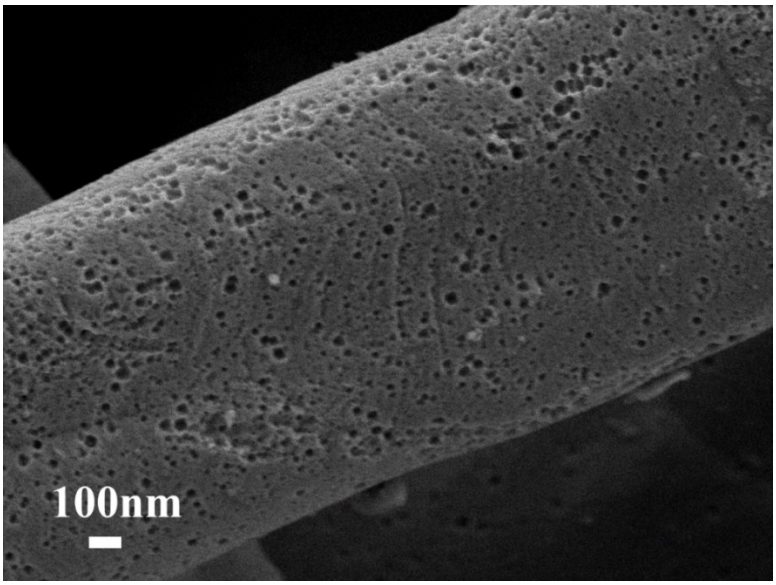

(b)

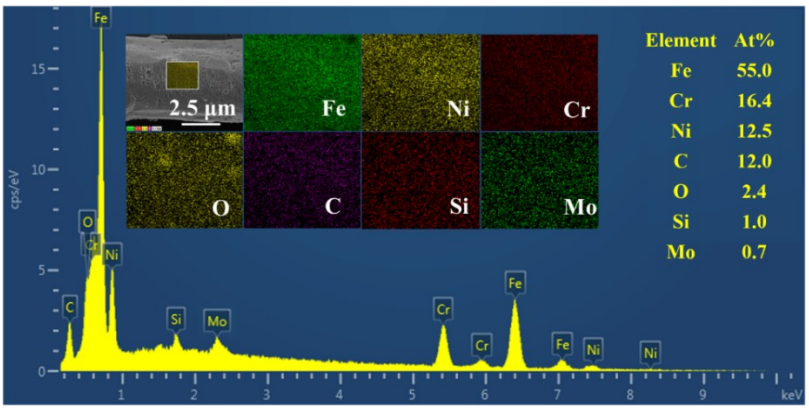

(c)

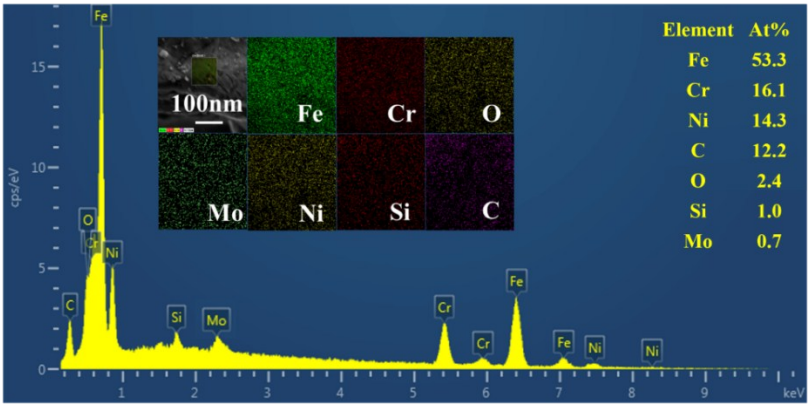

Figure S2 SEM image of the bare SS (**a**), EDS and the corresponding elemental mappings for the bare SS within two randomly selected areas (**b, c**).

Table S1 The atom % in the bare SS and K-doped FeOOH/Fe_3O_4/SS sample before and after electrochemical measurements.

Atom %	Bare SS	K-doped FeOOH/Fe_3O_4/ SS before GCD cycles	K-doped FeOOH/Fe_3O_4/ SS after 10000 GCD cycles	K-doped FeOOH /SS	FeOOH /SS
Fe	55.0 [a] /53.3 [b]	36.3 [c] /43.3 [d]	42.4 [e]	26.6 [f]	40.9 [g]
C	12.0 [a] /12.2 [b]	25.2 [c] /13.2 [d]	18 [e]	20.8 [f]	11.8 [g]
O	2.4 [a] /2.4 [b]	15.9 [c] /19.7 [d]	18.6 [e]	41.6 [f]	24.3 [g]
Ni	12.5 [a] /14.3 [b]	11.4 [c] /11.9 [d]	7.9 [e]	5.7 [f]	11.0 [g]
Cr	16.4 [a] /16.1 [b]	8.9 [c] /10.0 [d]	11.8 [e]	3.4 [f]	10.3 [g]
Mo	0.7 [a] /0.7 [b]	1.4 [c]	/	/	/
Mn	/	1.1 [d]	1.2 [e]	/	0.8 [g]
Si	1.0 [a] /1.0 [b]	0.8 [c] /0.7 [d]	/	0.3 [f]	0.4 [g]
K	/	0.1 [c] /0.1 [d]	0.1 [e]	1.5 [f]	/
S	/	/	/	0.2 [f]	0.5 [g]

[a] The percentages of the atoms are calculated based on the EDS data in Figure S2b;

[b] The percentages of the atoms are calculated based on the EDS data in Figure S2c;

[c] The percentages of the atoms are calculated based on the EDS data in Figure 2b;

[d] The percentages of the atoms are calculated based on the EDS data in Figure 2c;

[e] The percentages of the atoms are calculated based on the EDS data in Figure 8a;

[f] The percentages of the atoms are calculated based on the EDS data in Figure S14a;

[g] The percentages of the atoms are calculated based on the EDS data in Figure S14b.

(a)

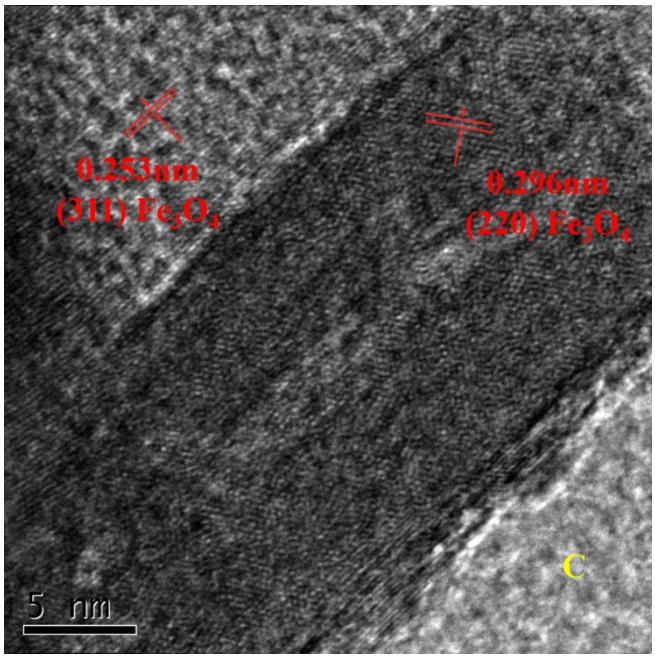

(b)

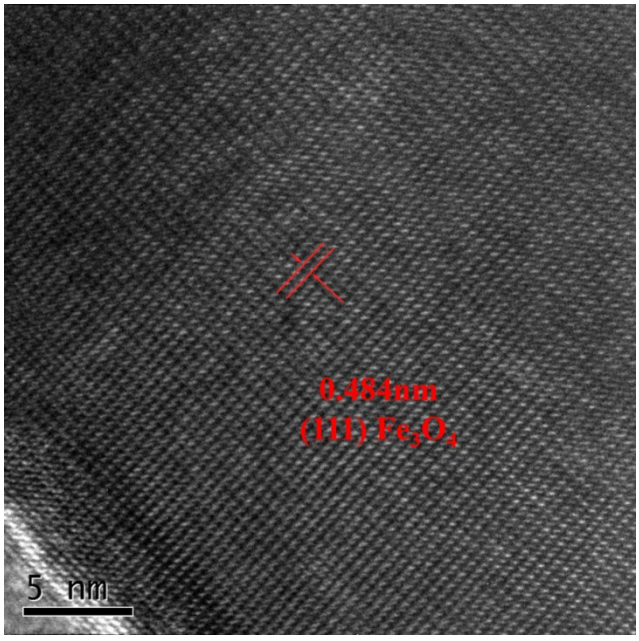

(c)

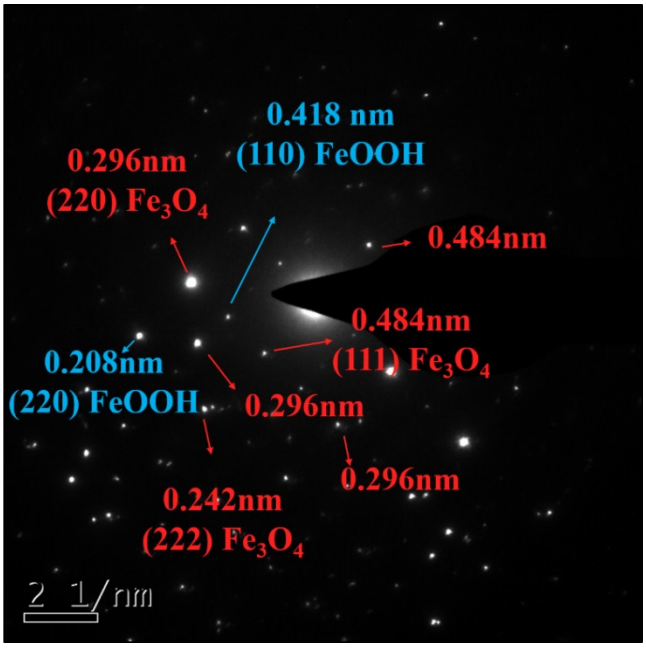
0.418 nm
(110) FeOOH
0.296nm
(220) Fe_3O_4
0.484nm
0.484nm
(111) Fe_3O_4
0.208nm
(220) FeOOH
0.296nm
0.296nm
0.242nm
(222) Fe_3O_4
2 1/nm

(d)

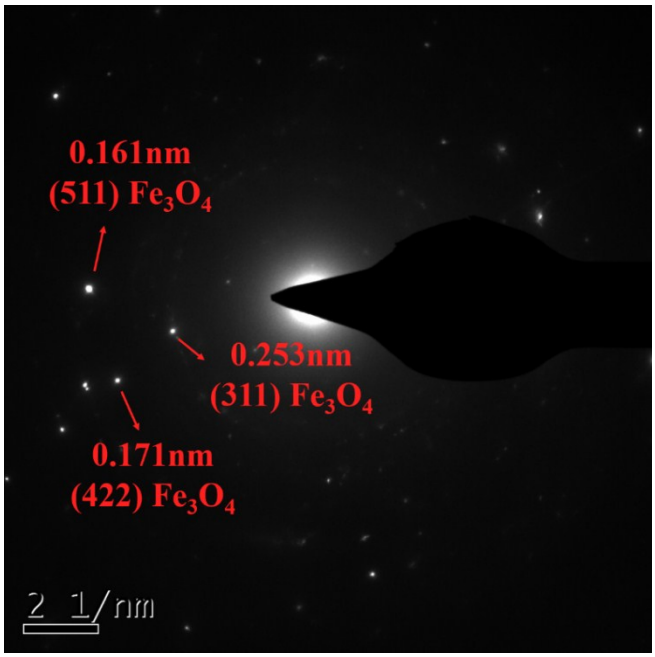
0.161nm
(511) Fe_3O_4
0.253nm
(311) Fe_3O_4
0.171nm
(422) Fe_3O_4
2 1/nm

(e)

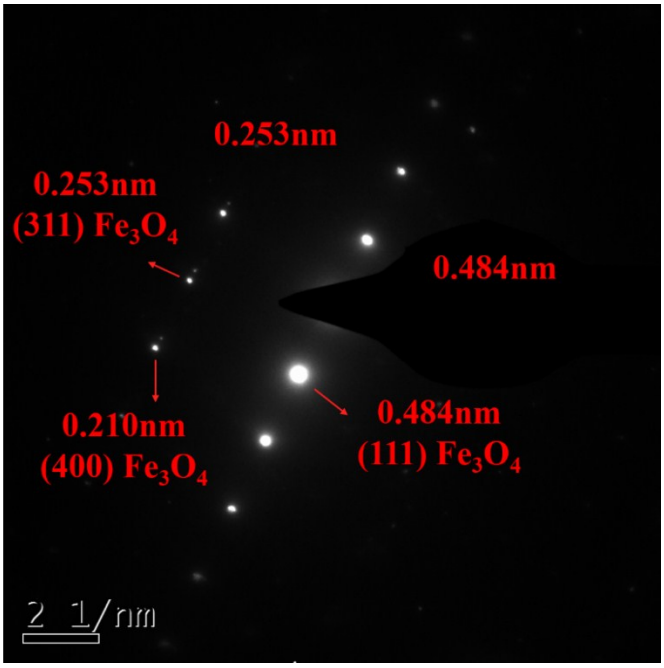

Figure S3 HRTEM **(a, b**) and SAED images (**c-e**) for K-doped FeOOH/Fe_3O_4/SS nanocomposite.

(a)

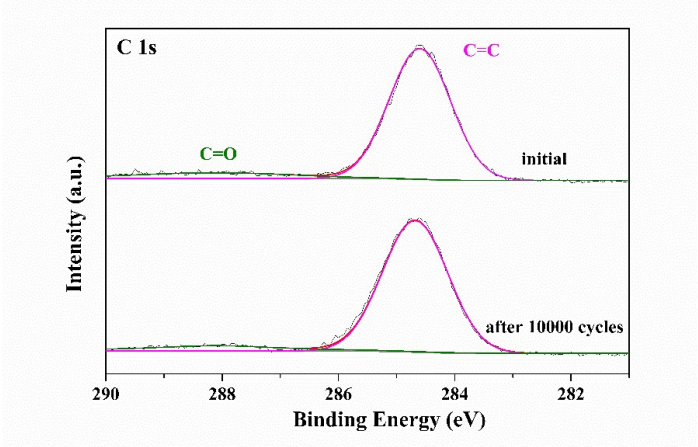

(b)

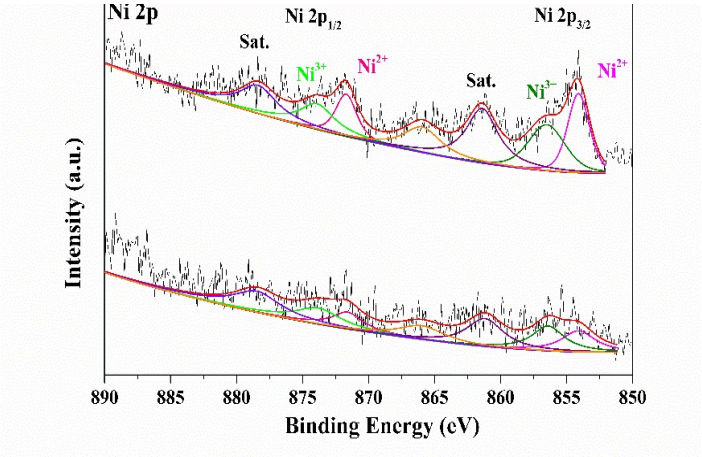

(c)

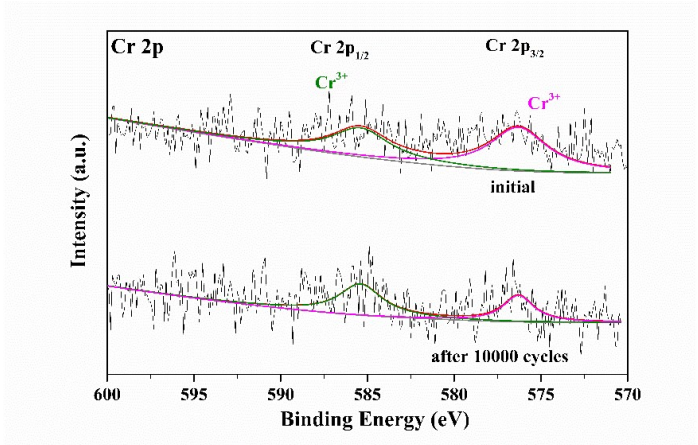

Figure S4 The XPS fine spectra of C 1s (a), Ni 2p (b) and Cr 2p (c) for K-doped FeOOH/Fe_3O_4/SS before (above) and after (below) 10000 GCD cycles.

(a)

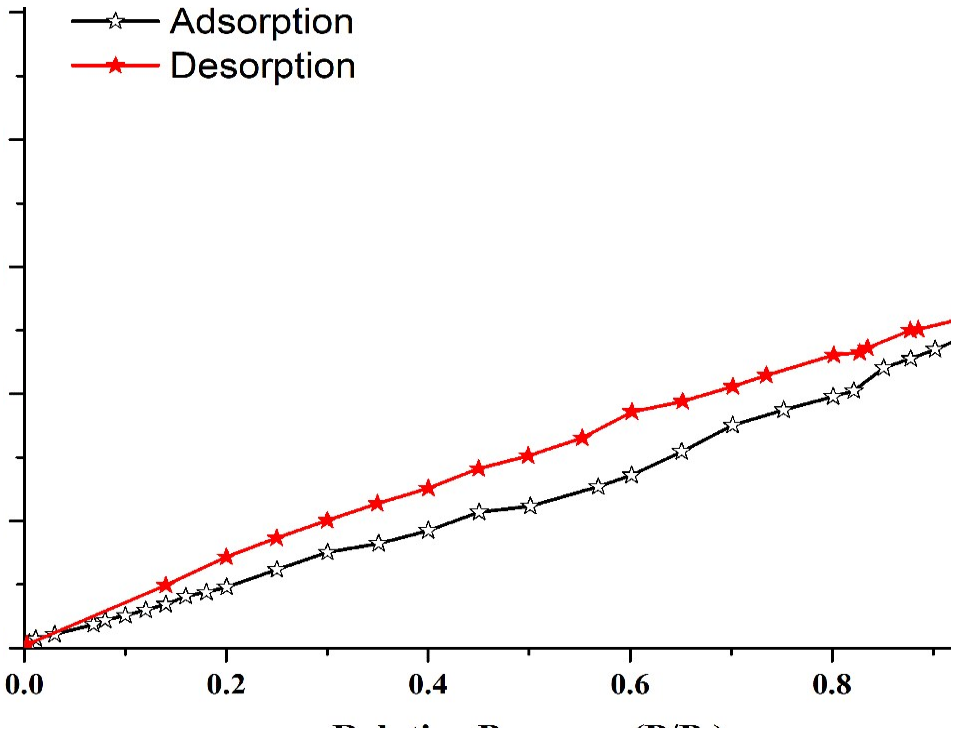

(b)

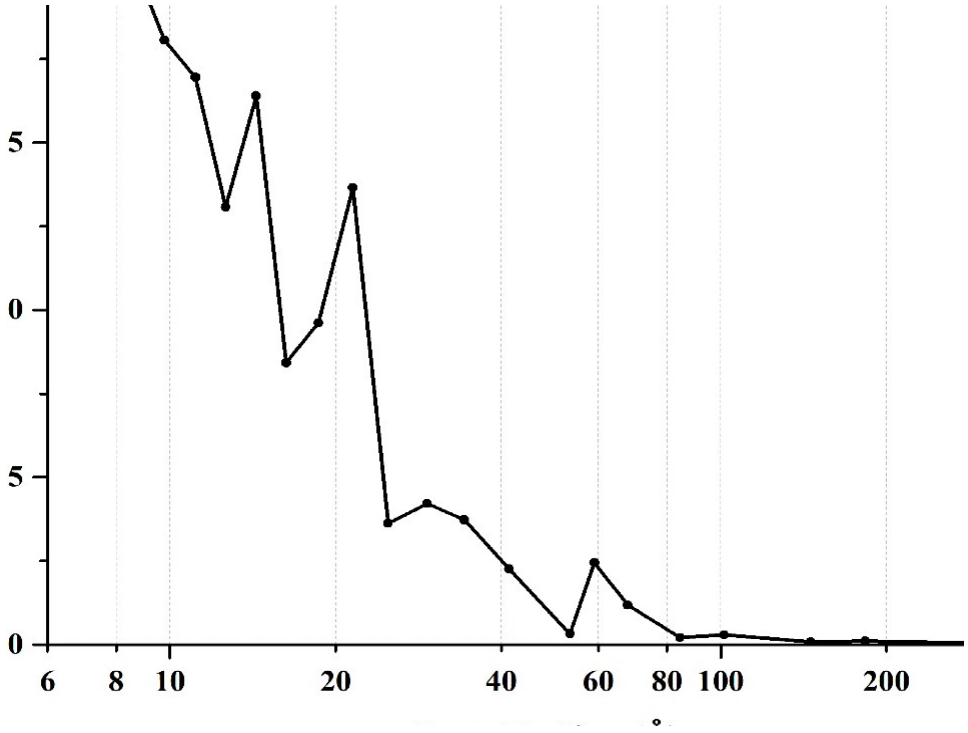

Figure S5 Nitrogen adsorption-desorption isotherms (**a**) and pore size distribution (**b**) curves of K-doped Fe_3O_4@FeOOH/SS.

(a)

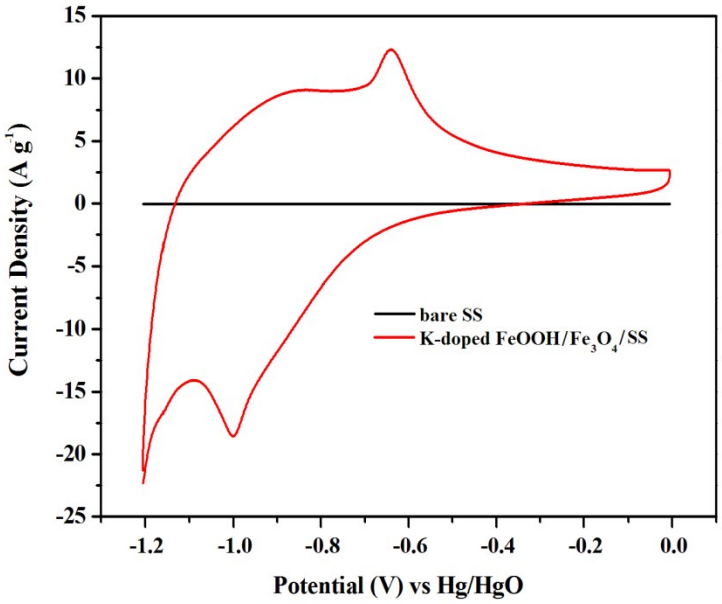

(b)

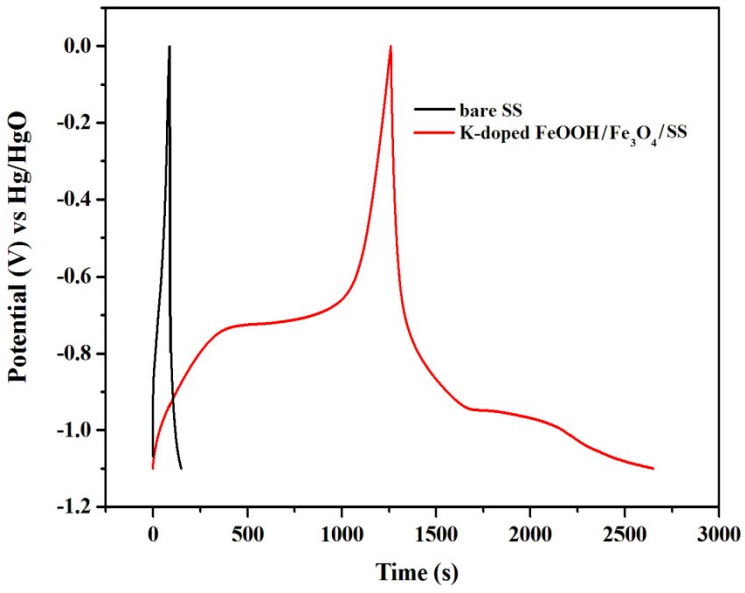

Figure S6 CV at 10 mV s^{-1} (**a**) and GCD curves at 1 A g^{-1} (**b**) for the bare SS and K-doped Fe_3O_4/FeOOH/SS.

Table S2 The electrochemical behaviors for iron oxides/hydroxides based anode materials reported previously.

Sample	Electrolyte	Current density ($A\ g^{-1}$)	Specific capacity ($F\ g^{-1}$)	Energy density	Capacity retention	Ref.
FeOOH/C	6 M KOH	0.5	396	/	/	1
Dy^{3+}-doped Fe_3O_4	1 M Na_2SO_4	0.5	202	/	/	2
α-Fe_2O_3/rGO	1 M KOH	1	903	/	/	3
Fe_3O_4 NRs/NH_2-rGO	1 M Na_2SO_4	1	145	/	/	4
Fe_3C/Fe_3O_4/C	6 M KOH	0.5	315	/	/	5
(AC)-Fe_3O_4	6 M KOH	0.5	37.9	/	/	6
Fe_2O_3/N-rGO	1 M KOH	0.5	618	/	/	7
Fe_2O_3 NDs@NG	2 M KOH	1	274	/	/	8
FeO_x-CNFs	6 M KOH	1	460	/	/	9
FeOOH QDs	1 M Li_2SO_4	1	365	/	/	10
α-Fe_2O_3/C	1 M Na_2SO_4	1	391.8	0.64 mWh cm^{-3} at 14.8mW cm^{-3}	71.8% (4000 cycles at 200 mV s^{-1})	11
PEDOP@Fe_3O_4 NSs	1 M $LiClO_4$/PC/ 15 wt% PMMA based gel	1	673	93 Wh kg^{-1} at 0.5 kW kg^{-1}	83% (5000 cycles at 1 A g^{-1})	12
Fe_2O_3/MWCNTs	1 M Na_2SO_4	2	437.5	38 Wh kg^{-1} at 800 W kg^{-1}	65 % (500 cycles at 2 A g^{-1})	13
G@Fe_3O_4	2 M KOH	2	732	82.8 Wh kg^{-1} at 2047 W kg^{-1}	88.3% (10000 cycles at	14

					20 A g^{-1})	
Fe_3O_4@C	6 M KOH	0.5	586	18.3 Wh kg^{-1} at 351 W kg^{-1}	66.7% (1000 cycles at 5 A g^{-1})	15
Fe_3O_4@CNF_{Mn}	Gel Na_2SO_4/PVA	1	306	13 Wh kg^{-1} at 65 W kg^{-1}	85% (2000 cycles at 0.5 A g^{-1})	16
MnO_2@Fe_2O_3	Gel Na_2SO_4/CMC	0.69	91	41.8 Wh kg^{-1} at 1276 W kg^{-1}	91% (3000 cycles at 100 mV s^{-1})	17
FeOOH	2 M KOH	1	1066	104 Wh kg^{-1} at 1.27 kW kg^{-1}	91% (10000 cycles at 30 A g^{-1})	18
FeOOH/RGO	1 M Li_2SO_4	1	142.0	16 Wh kg^{-1} at 0.6 kW kg^{-1}	90% (1000 cycles at 40 A g^{-1})	19
Co−Fe_3O_4 NS@NG	3 M KOH	1	775	89.1 Wh kg^{-1} at 0.901 kW kg^{-1}	97.1% (10000 cycles at 1 A g^{-1})	20
K-doped FeOOH/Fe_3O_4/SS	2 M KOH	1	1296 (396 mAh g^{-1})	74.38 Wh kg^{-1} at 3.64 W kg^{-1}	85.6 % (3000 cycles at 30 A g^{-1})	This work

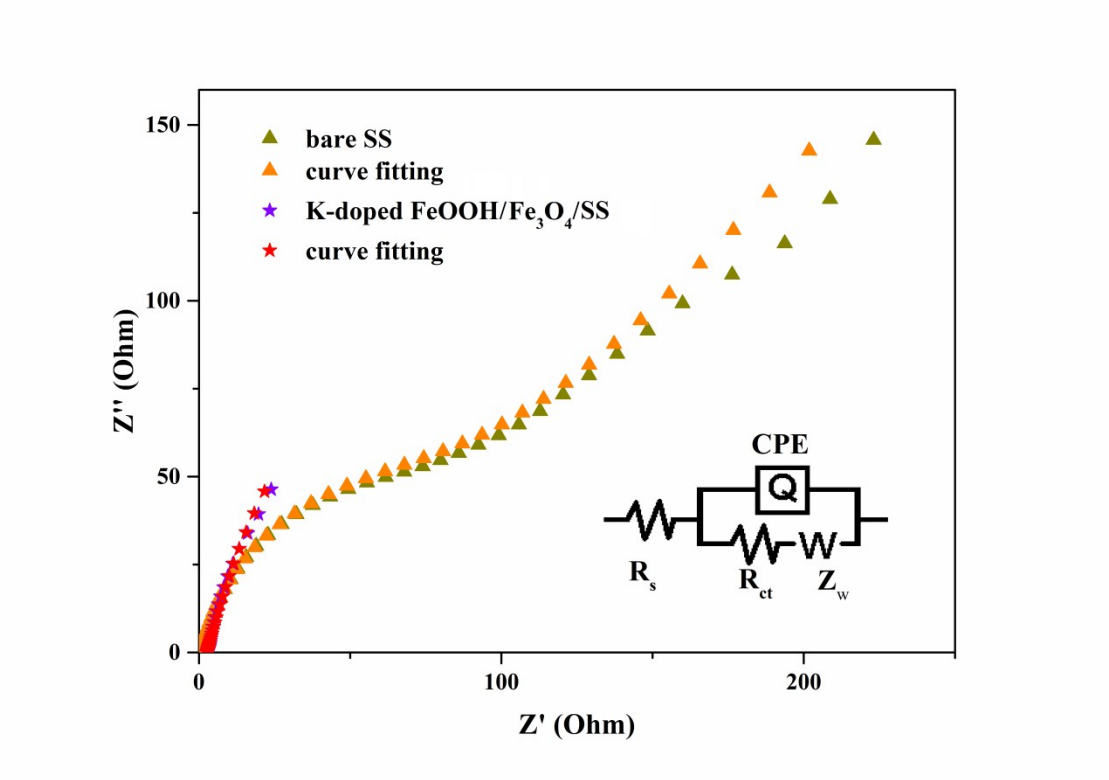

Figure S7 Niquist plots for the bare SS and K-doped FeOOH/Fe_3O_4/ SS

Table S3 Parameters obtained from the simulation of the Nyquist plots for the bare SS and K-doped FeOOH/Fe_3O_4/SS before and after 5000/10000 GCD cycles.

Sample	R_{ct}**(Ω cm^{-2})**	R_s**(Ω cm^{-2})**
bare SS	85.3	0.9698
K-doped FeOOH/Fe_3O_4/SS	376.8	2.754
K-doped FeOOH/Fe_3O_4/SS after 5000 GCD cycles	49.1	0.8743
K-doped FeOOH/Fe_3O_4/SS after 10000 GCD cycles	92.1	1.038

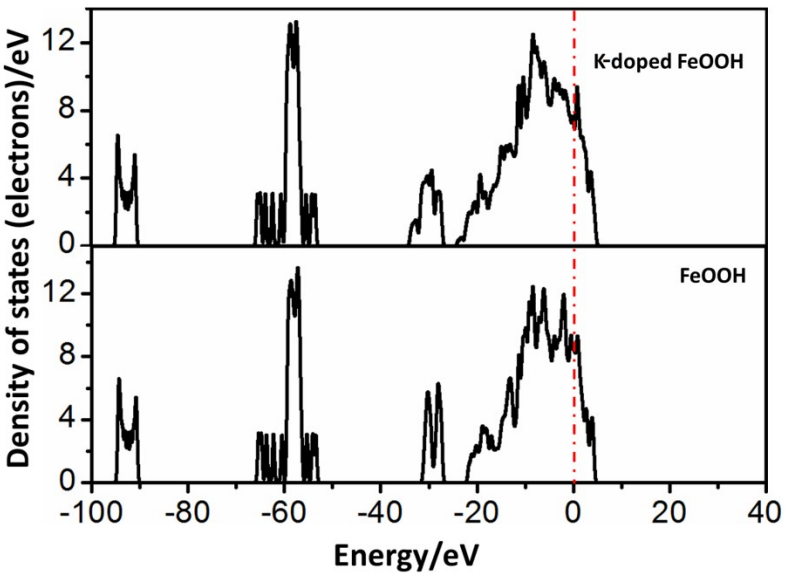

Figure S8 The comparative TDOS for the K-doped and –undoped FeOOH.

(a) **(b)**

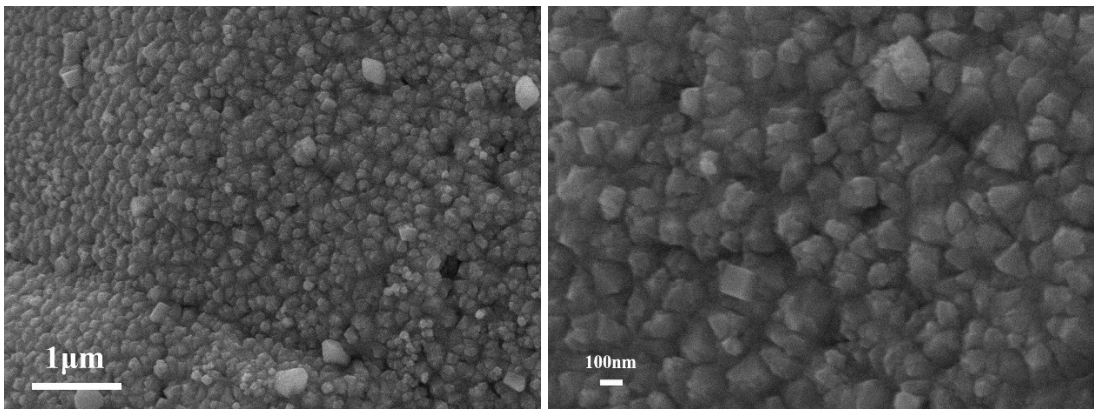

(c) **(d)**

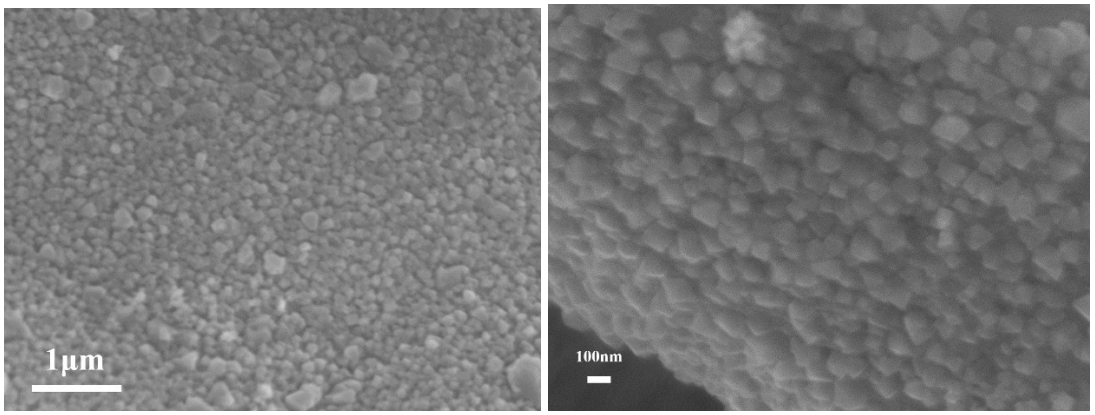

(e) **(f)**

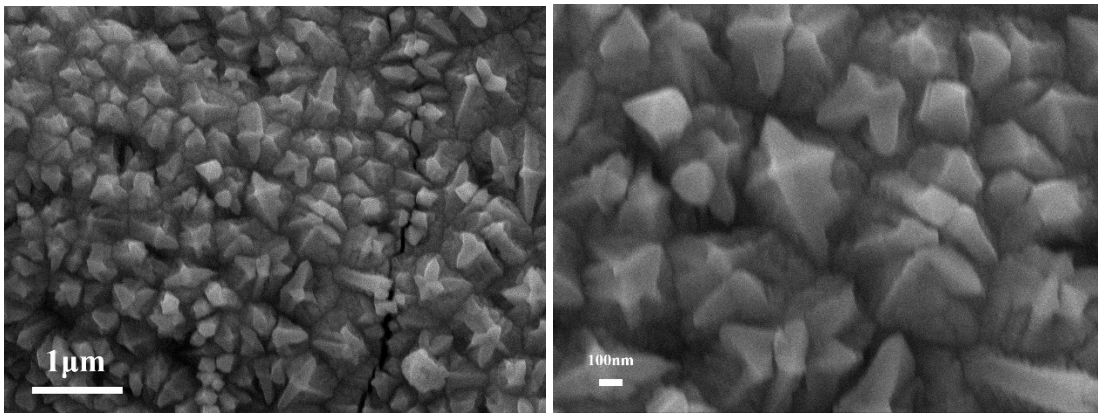

Figure S9 SEM images of K-doped FeOOH/Fe_3O_4/SS composites prepared under different reaction temperatures: 140 ℃ (**a, b**), 160 ℃ (**c, d**) and 180 ℃ (**e, f**).

(a)

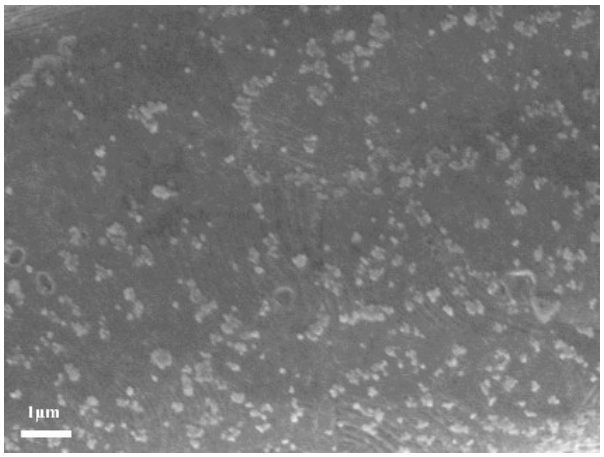

(b)

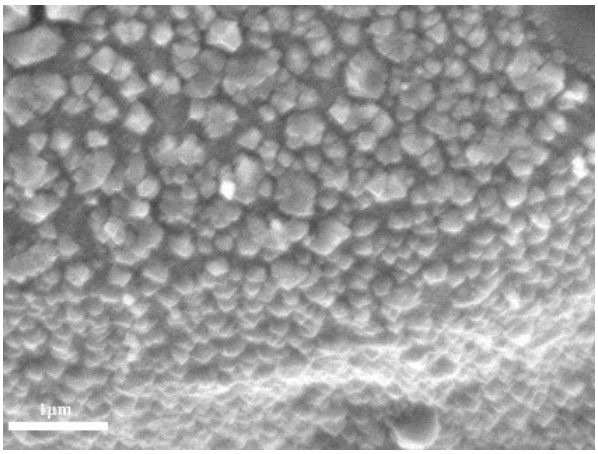

(c)

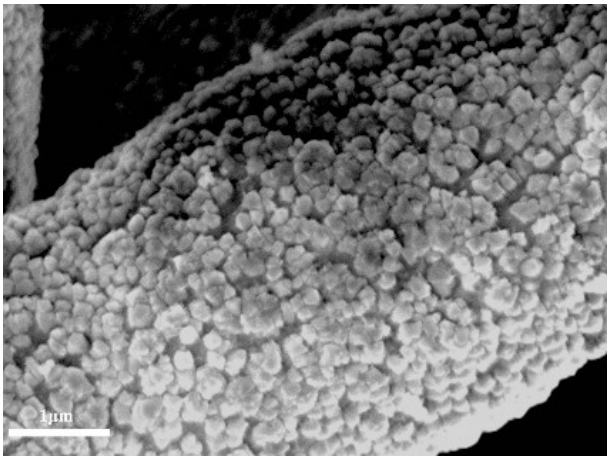

Figure S10 SEM images of K-doped FeOOH/Fe_3O_4/SS composites prepared with different amounts of KOH: 0.50 mmol (**a**), 0.75 mmol (**b**) and 1.00 mmol (**c**).

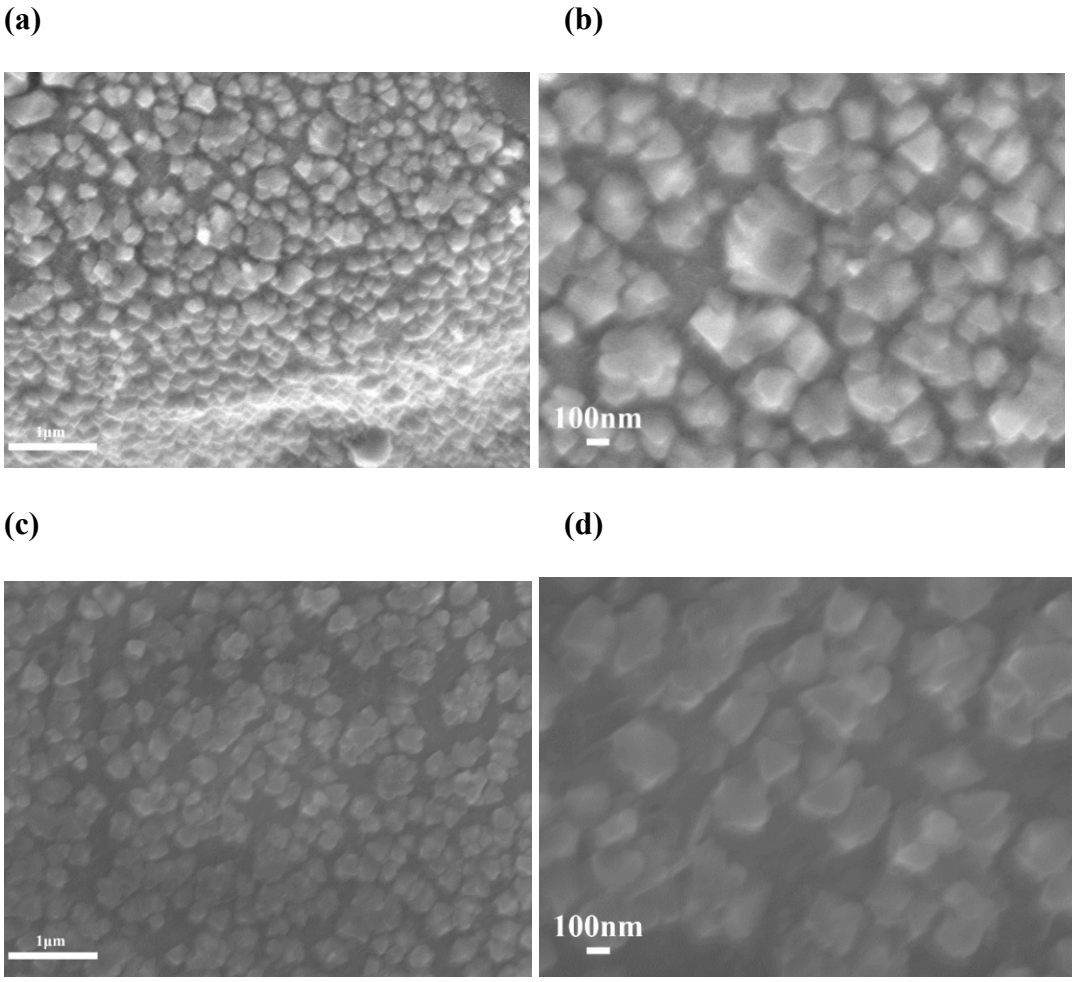

Figure S11 SEM images of K-doped FeOOH/Fe_3O_4/SS composites prepared under different reaction times: 12 h (**a, b**) and 24 h (**c, d**).

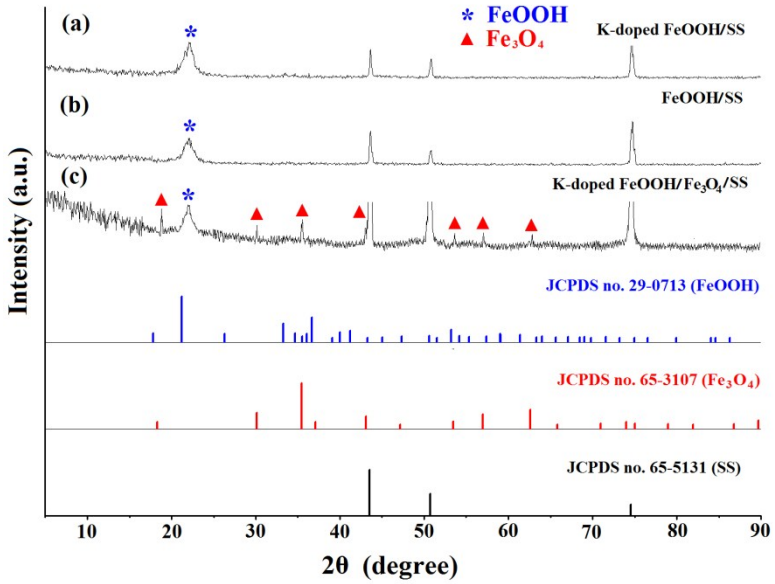

Figure S12 XRD patterns of the samples prepared in the absence of H_2O_2 (**a**) or KOH (**b**) in comparison with K-doped FeOOH/Fe_3O_4/SS (**c**).

(a)

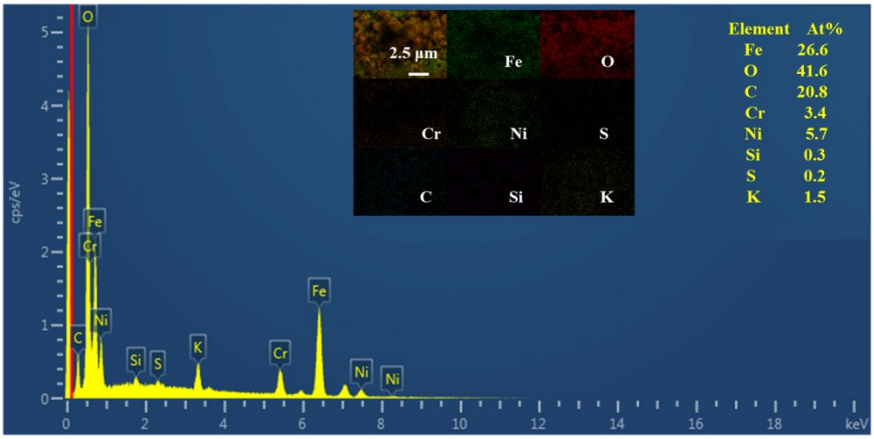

(b)

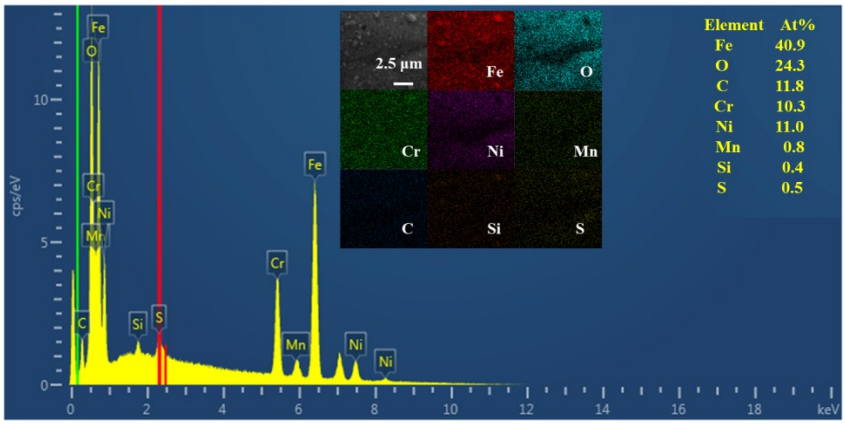

Figure S13 EDS and elemental mapping images of K-doped FeOOH/SS (**a**) and FeOOH/SS (**b**) prepared in the absence of H_2O_2 or KOH, respectively.

(a) **(b)**

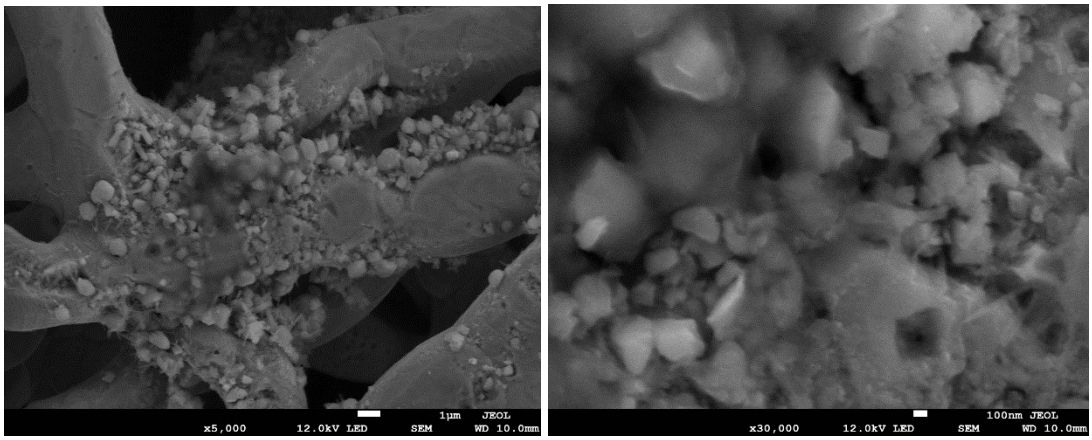

(c) **(d)**

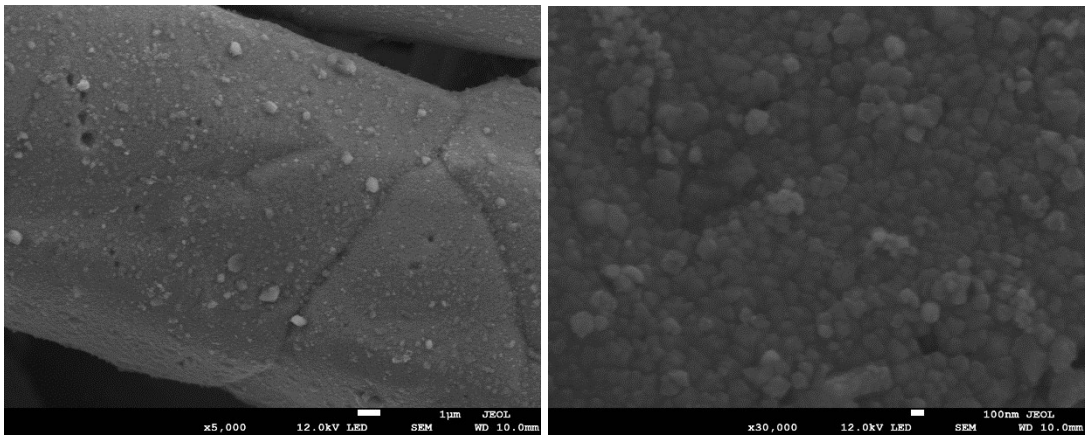

(e) **(f)**

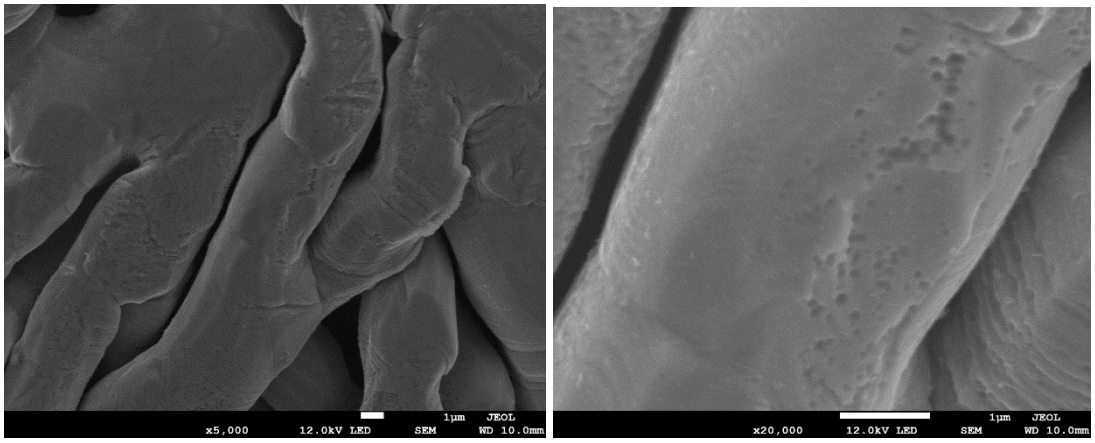

Figure S14 SEM images K-doped FeOOH/SS (**a, b**) and FeOOH/SS (**c-f**).

(a)

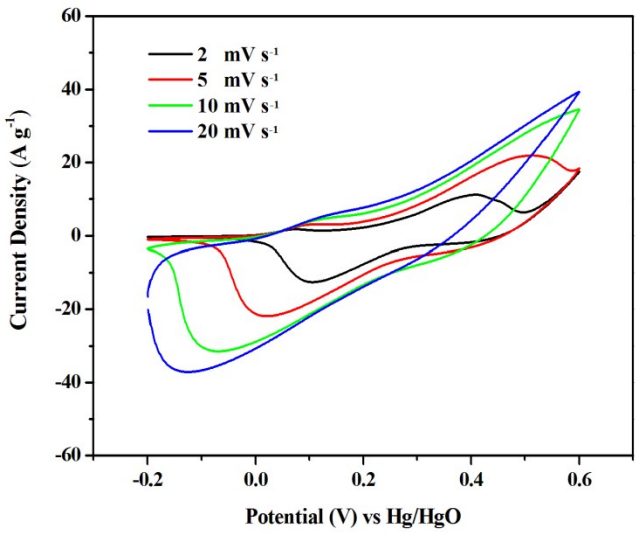

(b)

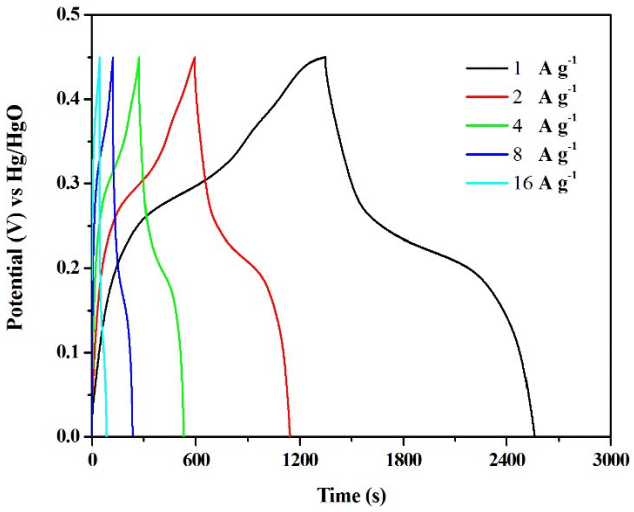

Figure S15 CVs at different scan rates (**a**) and GCD curves at different current densities for Co-Mo-O/Ni_3S_2/NF (**b**).

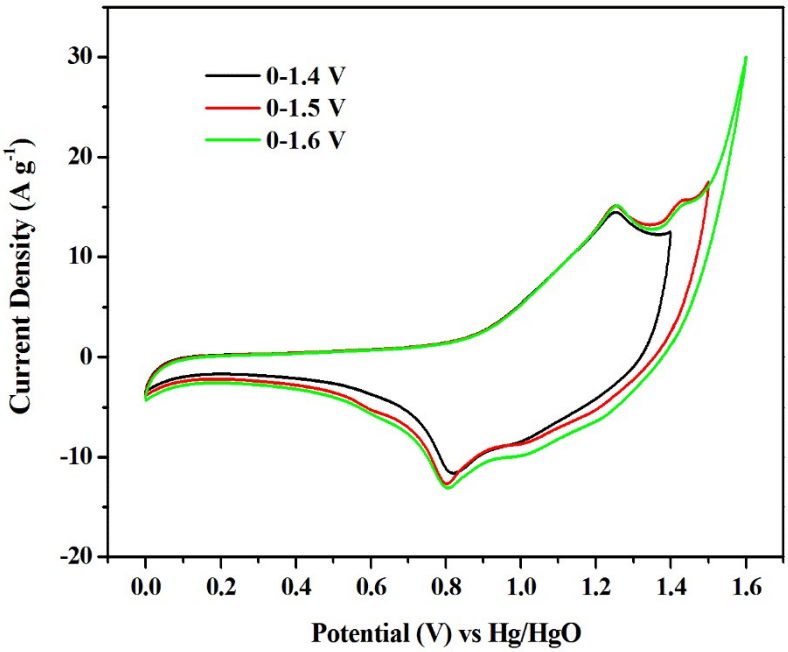

Figure S16 CV curves of the Co-Mo-O/Ni_3S_2/NF // K-doped FeOOH/Fe_3O_4/SS device at 20 mV s^{-1} in different voltage windows.

Reference

1. M. Aghazadeh and M. R. Ganjali, *Ceramics International*, 2018, **44**, 520-529.
2. J. Li, D. Chen, Q. Wu, X. Wang, Y. Zhang and Q. Zhang, *New Journal of Chemistry*, 2018, **42**, 4513-4519.

3. D. Chen, S. Zhou, H. Quan, R. Zou, W. Gao, X. Luo and L. Guo, *Chemical Engineering Journal*, 2018, **341**, 102-111.
4. F. Zhu, *International Journal of Electrochemical Science*, 2017, **12**, 7197-7204.
5. L. Yao, J. Yang, P. Zhang and L. Deng, *Bioresource Technology*, 2018, **256**, 208-215.
6. X. Du, C. Wang, M. Chen, Y. Jiao and J. Wang, *The Journal of Physical Chemistry C*, 2009, **113**, 2643-2646.
7. Z. Ma, X. Huang, S. Dou, J. Wu and S. Wang, *The Journal of Physical Chemistry C*, 2014, **118**, 17231-17239.
8. L. Liu, J. Lang, P. Zhang, B. Hu and X. Yan, *ACS Applied Materials & Interfaces*, 2016, **8**, 9335-9344.
9. R. Pai, A. Singh, S. Simotwo and V. Kalra, *Advanced Engineering Materials*, 2018, **0**, 1701116.
10. J. Liu, M. Zheng, X. Shi, H. Zeng and H. Xia, *Advanced Functional Materials*, 2015, **26**, 919-930.
11. H. Quan, B. Cheng, Y. Xiao and S. Lei, *Chemical Engineering Journal*, 2016, **286**, 165-173.
12. B. N. Reddy, S. Deshagani, M. Deepa and P. Ghosal, *Chemical Engineering Journal*, 2018, **334**, 1328-1340.
13. S. S. Raut and B. R. Sankapal, *New Journal of Chemistry*, 2016, **40**, 2619-2627.
14. J. Lin, H. Liang, H. Jia, S. Chen, J. Guo, J. Qi, C. Qu, J. Cao, W. Fei and J. Feng, *Journal of Materials Chemistry A*, 2017, **5**, 24594-24601.
15. H. Fan, R. Niu, J. Duan, W. Liu and W. Shen, *ACS Applied Materials & Interfaces*, 2016, **8**, 19475-19483.
16. N. Iqbal, X. Wang, A. A. Babar, G. Zainab, J. Yu and B. Ding, *Scientific Reports*, 2017, **7**, 15153.
17. G. S. Gund, D. P. Dubal, N. R. Chodankar, J. Y. Cho, P. Gomez-Romero, C. Park and C. D. Lokhande, *Scientific Reports*, 2015, **5**, 12454.
18. K. A. Owusu, L. Qu, J. Li, Z. Wang, K. Zhao, C. Yang, K. M. Hercule, C. Lin, C. Shi, Q. Wei, L. Zhou and L. Mai, *Nature Communications*, 2017, **8**, 14264.
19. H.-W. Chang, C.-L. Dong, Y.-R. Lu, Y.-C. Huang, J.-L. Chen, C. L. Chen, W.-C. Chou, Y.-C. Tsai, J.-M. Chen and J.-F. Lee, *ACS Sustainable Chemistry & Engineering*, 2017, **5**, 3186-3194.
20. M. Guo, J. Balamurugan, X. Li, H. Kim Nam and H. Lee Joong, *Small*, 2017, **13**, 1701275.